PAPER • OPEN ACCESS

Strength analysis of 3D printed carbon fibre reinforced thermoplastic using experimental and numerical methods

Strength analysis of 3D printed carbon fibre reinforced thermoplastic using experimental and numerical methods

F Ghebretinsae*, O Mikkelsen and A D Akessa

Department of Mechanical and Structural Engineering and Materials Science, University of Stavanger, Stavanger, Norway

* Corresponding author: f.ghebretinsae@stud.uis.no

Abstract. A study of strength of composite materials produced by 3D printing technology is presented. The samples fabrication and tests to determine the strength both in bending and in tension of the composite materials have been carried out. The composite samples were additively manufactured using Markforged® 3D printer of type Mark-Two. The fabricated composite samples were of carbon fiber filament combined with a thermoset plastic matrix, by its producer named "Onyx". The tests provided sample mean value for the ultimate tensile strength of 560 MPa and the tensile modulus of 25 GPa. Based on the three point bending tests the ultimate flexural strength of 271 MPa and flexural modulus of 16 GPa were estimated. The tests are reported and discussed in view of stress analysis modeling the layered composite with finite element models.

1. Introduction

Additive Manufacturing (AM) is defined as manufacturing of a component by laying a material layer upon a layer [1]. It is one of the currently developing method of manufacturing process [2]. Fast fabrication of prototypes using AM reduces product development time significantly. Prototypes make communication easier by "touch and feel" type of communication. Specially 3D printing has a great advantage due to 3D models can be fabricated without geometrical limitations and no additional machines/tools are required [2]. However, products fabricated with 3D printing have size limitations due to the capability of the 3D printer. 3D printed products have anisotropic mechanical properties and are more porous than traditionally manufactured products [3, 4]. In this study the terms such as '3D printer' referrers specifically to the 3D AM machine and '3D printing' to the AM processes by 3D printers.

Laying continuous reinforcing fiber within a matrix has been commonly practiced in traditional manufacturing of parts from composite materials in aerospace and automobile industries [5, 6]. However, the use of composite materials in AM occurs to be relatively new and it significantly increases the structural applicability of parts fabricated by AM [2]. The introduction of composite materials to AM takes the technology from prototyping stage further to the fabrication of strong functional parts. However, there is limited understanding of mechanical property of parts produced by AM and their mechanical property depends on; the building direction [7], layer-thickness [3, 8], bonding strength between layers [8], formation of voids [9], type of materials [8], etc. A unique advantage of AM when used for composite materials is that the orientation and alignment of continuous fiber can be located accurately in complex geometries, which is extremely challenging in traditional molding fabrication.

Composite materials have high strength to weight ratio, high corrosion and wear resistance, good fatigue life and thermal conductivity [10]. These properties make composite materials attractive in engineering applications. Composites have anisotropic material properties ($E_{11} \neq E_{22} \neq E_{33}$). However, by applying fiber in different orientation at each layer a "quasi-isotropic" property can be achieved [5, 11]. Furthermore, the fiber provides maximum strength when load is applied in the direction of the fiber, whereas the loads applied perpendicular to the fiber mostly depend on the weak matrix phase [12]. The term "fiber" is used in synonym to the strengthening material in this study. The strength and stiffness of the composite materials is mainly dependent on the type and volume fraction of the reinforcing phase, angle of orientation and fabrication method [3, 9, 10, 13]. Basically, higher fiber volume fraction provides higher strength and stiffness. However, to obtain adequate matrix support to the fiber, the volume percentage of the reinforcement should be less than 70% of the total volume of a component [14]. Elastic modulus in the longitudinal direction for a continuous and unidirectional (UD) fiber reinforced composite can be expressed by the 'Rule of Mixtures' (ROM). The rule shows that "the stiffness of the composite material is a weight-mean of the modulus of the two phases and simply depends on the volume fraction of fibers" [1].

$$E_c = E_m V_m + E_f V_f \qquad (1)$$

Where E stands for the E-modulus, V stands for the volume fraction. Whereas the subscripts c stands for the composite part, m for the matrix and f for the fiber (strengthening) phase. A similar equation to Equation (1) can be used to predict the stress, density, Poisson's ratio and shear strength.

Lozada, J.N. et al. studied effect of density and type of infill patterns on the stiffness and strength of Nylon and Onyx and found that both properties increased with increasing density. However, among all types of patterns, the triangular pattern provide best strength per weight result [13]. Moreover, Ning et al, studied the effect of printing parameters such as infill-speed, nozzle temperature and layer thickness and found that thicker layers led to largest average strength, while high nozzle temperature increased porosity [3]. Generally, both the AM parameters and fiber orientation influence the mechanical property of finished composite part [15].

For numerical simulation, composite material can be modelled using layer elements. After creating a model using layered elements, structural analysis including large deflection and stress can be performed [16]. It is important to take special attention when modeling composite materials due to finite element analysis (FEA) of composites require several orthotropic material properties [16]. At least two materials and nine orthotropic properties of each material are required. The nine parameters are elastic moduli (E_1, E_2, E_3), shear moduli (G_{12}, G_{23}, G_{31}), and Poisson's ratios (v_{12}, v_{23}, v_{31}) [16]. Subscripts 1, 2, and 3 represents x-, y- and z- directions, respectively.

2. Methodology
To characterize the mechanical properties of 3D printed composite materials, tensile and flexural experimental tests were performed following the ASTM D3039 and ASTM D7264-07 standards. Moreover, a finite element model was developed.

2.1. Markforged® Mark-Two 3D Printer
Mark-Two is the second generation desktop 3D-Printer for composite materials, introduced in 2016 by Markforged® [17]. Mark-two is a compact 3D printer which benefits from both the Fused Filament Fabrication (FFF) and Continuous Filament Fabrication (CFF) technology. Test samples were fabricated from carbon fiber (CF) filament and a thermoset plastic matrix, named "Onyx" [18], where both materials were delivered by Markforged®. In this report, "Onyx" is used as synonym to the matrix material. The 3D printer can also use Nylon as a matrix and fibers such as fiberglass (FG), Kevlar and high-strength high-temperature fiberglass (HSHT) [19].

Table 1. Slicing software (Eiger®) setting used when 3D printing test samples using Mark-Two.

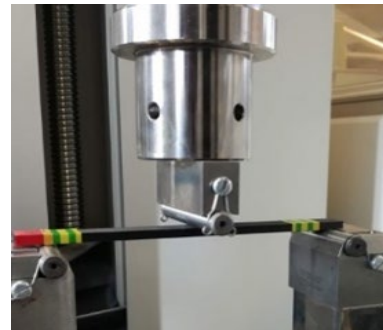| Description	Tensile Onyx/CF	Flexural Onyx/CF
Nozzle temperature	272 °C	272 °C
Heat bed temperature	No heat	No heat
Fill pattern	Solid	Solid
Fill density	100%	100%
Sample dimension [mm]	250x15x1.75	154x13x4
Floor layers	2	4
Roof layers	2	4
Layer thickness [mm]	0.125	0.125
Wall layers	1	2
Total fiber layers	10	20
Total matrix layers	4	12
Fiber fill type	Isotropic	Isotropic
Concentric fiber rings	1	1
Fiber angle (degrees)	0	0
Print time per pcs	2h 05min	1h 44min

The maximum size that can be built by mark Two is 320 mm x 132 mm x 154 mm (x-y-z respectively). Mark-Two has two nozzles where one nozzle is used for the matrix material and the second nozzle is used for the reinforcing fiber. The filament material is heated to its glass transition inside the nozzle and extrudes while the printer head move in the XY-plane. Only one nozzle at a time extrudes material and the continuous fiber is terminated at every layer. After one layer is deposited the working bed moves one-layer thickness along the z-direction as specified in the slicing software, which is 0.125 mm if CF is used. This thickness is pre-defined when printing parts with reinforcing fiber. Unlike other AM machines, the working bed of Mark-two do not need heating and parts can be removed right after fabrication is finished. The 3D printer settings used in this study are summarized in Table 1.

2.2. Tensile Test and sample preparation
Hart et al. [7] performed tensile test on dog-bone shaped CF reinforced composite fabricated by 3D printing and failure occurred at the grip section in all the samples. It was later recommended rectangular specimen with bonded tabs of standard type ASTM D3039. The tensile test in this study was performed following this recommendation and ASTM D3039 standard for tensile test of composite materials was used.

a)   Tensile setup using Instron 5895.   b)   3-point flexural setup using Zwick/Z020.

Figure 1. Tensile and flexural setups using corresponding universal testing machine.

Five rectangular CF reinforced tensile specimen with 250 mm in length,15 mm in width and 1.75 mm in depth was loaded in tension by Instron-5895 testing machine at a constant strain rate of 0.008 min^{-1}. The standard states that the strain rate should be selected so as failure to occur within 1 to 10 min and 0.01 min^{-1} is suggested [20]. However, during the trial test, the suggested strain rate led to fast and sudden failure. To overcome this, a reduced strain rate of 0.008 min^{-1} was used. The sample was clamped to a fixed part of the testing machine at the bottom and to the movable head at the other end as shown on Figure 1(a). Load was applied parallel to the UD CF and the samples were loaded until complete failure. The extension of the specimen were measured by an extensometer with gauge length of 100 mm. The test was carried at room temperature and normal humidity. It was important to consider the thickness of a single layer when selecting the thickness of the test sample because it is impossible to fabricate layers less than the minimum thickness accepted by the 3D printer [20]. Detailed information of each layer and applied material for the tensile sample is provided on Table 2. Moreover, the tensile sample had total 14 layers at the gauge section, where ten of them was made from CF and the rest was Onyx. The continuous CF was UD, oriented at 0° (along the x-axis) inside Onyx. To avoid damage and residual stress from the griper, the specimens were provided with 15 mm wide, 56 mm long and 1.5 mm thick tabs, beveled at 5° towards the gauge section as shown on Figure 2 (a). The tabs were simply printed together with the rectangular samples only with the matrix material. About 62% fiber volume fraction was estimated at the gauge section. Moreover, a solid infill with 100% density was used to reduce formation of voids and achieve enough fiber volume fraction. Each sample took approximately 2 hours printing time to complete.

2.3. Flexural Test and sample preparation
The three point flexural test was performed by Zwick/Z020 testing machine following the ASTM standards D- 7264M – 07, procedure-A. Five specimens with 154 mm length, 13 mm width and 4 mm thick (Figure 3) was fabricated by Mark-two 3D printer from UD continuous CF and Onyx matrix. A span to thickness ratio of 32:1 was used when selecting dimensions from the standard. The testing sample was simply supported at two ends, 124 mm apart and a concentrated load, uniformly distributed along the width of the beam was applied at the mid-span (Figure 3 (b)) [21]. Samples had been tested until failure at a head speed of 1 mm/min.

The distribution of the CF layers in the flexural test samples were decided by considering the loading conditions of a classical beam from the general beam theory, wherein the neutral axis of the beam is theoretically unstressed. Therefore, no reinforcing fiber was provided at the center of the beam (Figure 3(b)). Detailed information about each layer and applied materials type are provided on Table 4. For a single specimen of 4 mm thick, a total of 32 layers each 0.125 mm thick were required. Furthermore, the flexural samples had an approximately 42% fiber volume fraction and the CF were symmetrically located with reference to neutral axis of the beam (Figure 3 (b)).

$$\sigma = \frac{3PL}{2bh^2} \qquad (2)$$

Where *σ* is stress at the mid-span, *P, L, b* and *h* represent the applied force, support span, initial beam width and initial thickness, respectively [21].
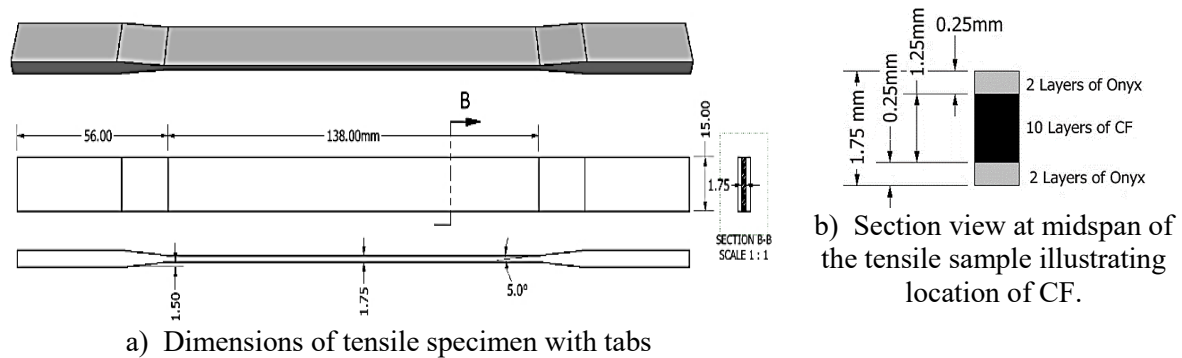
a) Dimensions of tensile specimen with tabs

b) Section view at midspan of the tensile sample illustrating location of CF.

Figure 2. Tabbed tensile test specimen.

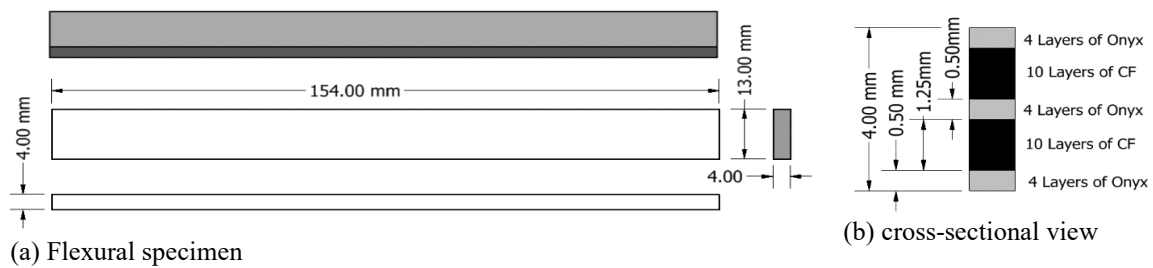(a) Flexural specimen

(b) cross-sectional view

Figure 3. Flexural specimen and detail section view of layers and assigned material.

2.4. Fiber volume fraction estimation

The total cross-sectional area was calculated by summing up the individual cross-sectional area covered by each material at the gauge section. The cross-sectional area was taken from a location within the gauge section. To find the fiber volume fraction the "rule of mixtures" were used. ROM uses the material properties of the individual composite materials and their volume ratio to predict the property of the composite part. Considering the matrix and fiber layer cover same length and width of the part, the volume fraction can be represented by area fraction equation (3).

$$V_f = \frac{A_f}{A} \ , \qquad V_m = \frac{A_m}{A} \tag{3}$$

$$E_c = E_m \frac{A_m}{A} + E_f \frac{A_f}{A} \tag{4}$$

Where A represents the total cross sectional area, while A_f and A_m stands for cross sectional area occupied by the fiber and matrix, respectively.

Considering Figure 3 (b) & 2 (b), and the approximated width of a single printed carbon filament, the area covered by CF was estimated .The area calculated was assumed to be at the middle of gauge length and the average dimension values of the printed sample were used on both tests. Moreover, the thickness of the layers was obtained by dividing the final thickness by the total number of layers in the sample. In similarity to the FE models, the presence of voids was ignored when estimating the fiber percent. From the 3D model and final printed sample dimensions the tensile and the flexural samples had a cross-sectional area increase of 7% and 1%, respectively. However, porosity and distribution of voids within the CF and Onyx was not studied.

2.5. Modeling tensile and flexural samples in Ansys

ANSYS Mechanical APDL 17.0 were used as a tool to model and analyze the specimen models of composite materials. In this study element type SHELL181 4-node structural shell was used and the samples were considered as thin walled. Shell181 was selected due to shell elements allow to define layered composite of thin-walled structures [22]. The CF and Onyx composite specimens were modelled as a thin layered lamina. Since the layers fabricated in the 3D printer were made of either the reinforcing or the matrix material, the model was also designed to contain only one type of material per lamina. This means one layer was made of either only CF or Onyx. Material properties presented on Table 3 were used for the simulation of both models. During developing FE model there have been made several assumptions. The assumptions made were; Constituents show linear elastic behavior, the matrix (Onyx) has isotropic material properties, fibers are transversely isotropic, fiber-matrix has perfect bonding and no voids or defects present in the test samples. Moreover, a Laminate Stacking Sequence (LSS) was used to create the 0.125 mm thick laminas and material properties and its orientation were defined. The lay-up was made in similar way as in the 3D printer settings. Details LSS are provided on Table 2 for tensile and Table 4 for flexural.

2.5.1. Tensile model: A finite element model of 1.75 mm thick, 15 mm wide and 138 mm in length (represents only the gauge section) was modeled in ANSYS for the tensile analysis. The left end of the model had a fixed boundary condition with zero displacement in all possible movements, whereas negative 559.9 MPa uniformly distributed pressure was applied at the right end of the model. All boundary conditions (BC) were applied on a line. Furthermore, the model was meshed with an element size of 0.75 producing 3680 total elements. The tensile model has 20 elements along its width and it contains only one element throughout its thickness.

Table 2. Layer orientation and material for each lamina for the tensile specimens.

Layer number	Total number of layers	Material type	Layer thickness [mm]	Orientation Angle, [°]
13, 14	2 layers	Onyx	0.125	(+45°,-45°)2
3-12	10 layers	CF	0.125	(0°)10
1, 2	2 layers	Onyx	0.125	(+45°,-45°)2

2.5.2. Flexural model: A finite element model of 4 mm thick, 13 mm wide and 186 mm length was modeled in ANSYS. The FE-model had a zero displacement only in z-direction at the two supports and only in y-direction at the left end of the model (Figure 4). Whereas the right end was constrained with zero DOF in x- and y- direction. The supports was 124 mm apart and the model was extended from the supports by 31 mm to each side. A total force of 303 N, with 33.7 N to each nodes was applied at 9 nodes located at the mid-span of the beam. The model was meshed into 8 elements along its width, with refined mesh at the mid-span of the beam and contains one element throughout the thickness. Furthermore, the output of the stress analysis are based on settings for full integration with incompatible modes of the shell elements.
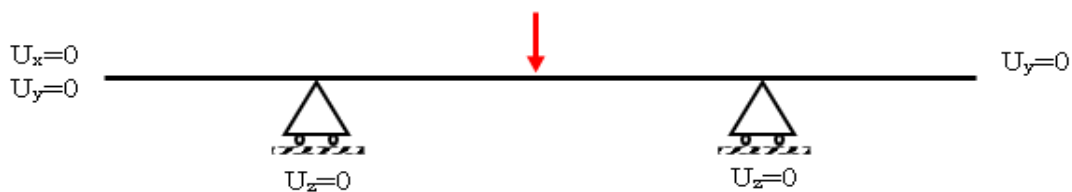

Figure 4. Boundary conditions for the flexural model.

2.5.3. Orthotropic material property assumption: van der Klift et al. [2] estimated the amount of fiber volume fraction on a single bundle of Markforged® carbon fiber filament by evaporating the matrix according to JIK K7075 and found a fiber volume fraction of 34.5% and the rest 65.5% was other coating and adhesive polymers. This estimation was used to calculate the assumed orthotropic material properties CF filament provided by Markforged® in this study. For making assumptions on the Poison's ratio of Onyx, five samples was tested and it is assumed be 0.43.

Table 3. Assumed material properties of Markforged® carbon fiber and Onyx used for simulation in Ansys. Typical AS4 CF yarn properties are adapted from Meddad, 2002 [23].

Description	AS4 carbon fiber yarn [23]	Markforged® CF		Data provided by
		Tensile	Flexural	
E-Modulus Onyx, [GPa]	-	1.4	2.9	Markforged®
Axial E-Modulus CF E11, [GPa]	231	54	51	Markforged®
Transverse E-Modulus CF E22= E33, [GPa]	22.4	7.728*	7.728*	Assumed
Axial Shear Modulus CF, G12= G13, [GPa]	22.1	7.625*	7.625*	Assumed
Transverse Shear Modulus, CF, G23, [GPa]	8.3	2.864*	2.864*	Assumed
Axial Poisson's Ratio , CF, v12= v13	0.3	0.104*	0.104*	Assumed
Transverse Poisson's Ratio, CF, v23	0.35	0.121*	0.121*	Assumed

Note: That values marked with * on Table 3 were obtained by considering only 34.5% of the AS4 CF values and unmarked values are provided by Markforged®.

Table 4. Layer orientation and material of each layer lamina of the flexural specimens. [1 is bottom layer and 32 is top layer].

| Layer number	Total number of Layers	Material type	Layer Thickness [mm]	Orientation Angle, [°]
29 - 32	4 layers	Onyx	0.125	(+45°,-45°)2
19 - 28	10 layers	CF	0.125	(0°)10
15 - 18	4 layers	Onyx	0.125	(+45°,-45°)2
5 - 14	10 layers	CF	0.125	(0°)10
1 - 4	4 layers	Onyx	0.125	(+45°,-45°)2

3. Results

The stress on experimental tensile test results is calculated by dividing the instantaneous force by the average initial cross-sectional area of the sample measured at the gauge section. Whereas the flexural stress is calculated using equation (2).

3.1. Results from tensile experimental test

The average maximum tensile strength obtained from the tensile samples was 560 MPa with a standard deviation (SD) of 17.70 MPa and tensile elastic modulus of 25 GPa with 2.7 GPa SD. The average yield strain was about 0.026 mm/mm. A stress-strain curve was generated from the individual tensile-test-sample results data and it is presented on Figure 5.

Table 5. Experimental results from tensile samples fabricated from CF and Onyx.

Description	Average Width [mm]	Average Thickness [mm]	Max. Load [kN]	Max Tensile Strength [MPa]	Tensile Modulus [GPa]	Tensile Strain [mm/mm]
S1	15.06	1.87	14.99	558.87	24.63	0.027
S2	14.98	1.86	15.07	537.75	20.59	0.032
S3	14.96	1.87	16.05	567.61	26.81	0.024
S4	14.98	1.88	15.40	550.37	26.27	0.025
S5	14.96	1.86	16.47	584.68	26.89	0.023
Mean	14.99	1.87	15.6	559.9	25	0.026
SD	0.04	0.01	0.64	17.72	2.65	0.004
CV [%]	0.3%	0.4%	4%	3%	11%	14%
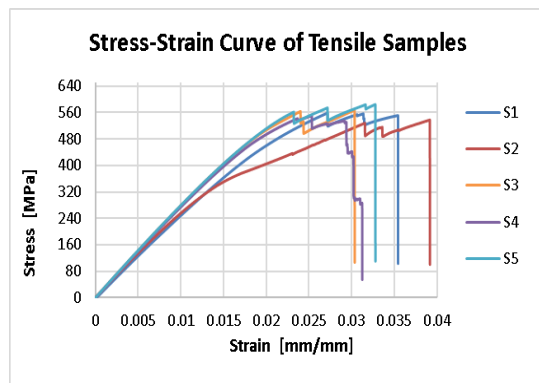
Figure 5. Stress-Strain curve of tensile specimens.

Figure 6. Failed UD tensile samples.

3.2. Experimental results from the 3-point flexural test
From the experiment, a maximum mean flexural strength of 271 MPa was obtained. Equation (2) was used to estimate the flexural stress and a stress strain curve is provided on Figure 7. Results from the flexural experimental test are provided on Table 6.

Table 6. Flexural 3-point test experimental results.

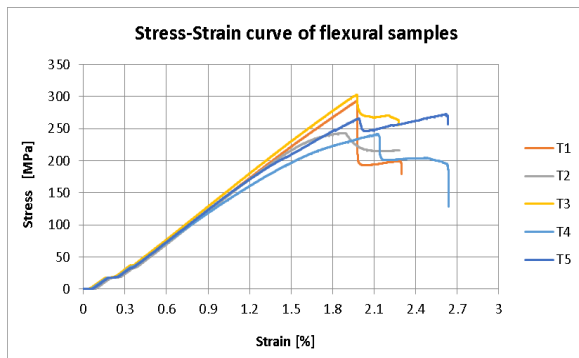| Description	Average width [mm]	Average Thickness [mm]	Max. Load [N]	Flexural Strength [MPa]	Flexural Modulus [GPa]	Flexural Strain [%]
T1	12.98	4.01	328.27	293.55	15.53	2.30
T2	12.97	4.04	271.58	242.86	16.17	4.19
T3	13.01	4.03	339.05	303.19	16.73	2.28
T4	12.96	4.04	270.26	241.68	18.56	2.64
T5	12.98	4.03	304.47	272.27	15.11	2.63
Mean	12.98	4.03	302.7	270.7	16.4	2.8
SD	0.02	0.01	31.62	28.27	1.35	0.79
CV [%]	0.14%	0.30%	10%	10%	8%	28%

Figure 7. Stress-Strain Curves of flexural Samples.

Figure 8. Failed three-point flexural sample.

3.3. FEA results from tensile model

From the FE-model, a nodal longitudinal displacement of 1.13 mm was determined. The longitudinal distribution of tensile stress in CF layer is shown in Figure 9, representing layer 7 of the finite elements. Apart from the steep tensile stress gradient close to the fixed boundary as presented in Figure 10 a uniform distributed axial stress of 443 MPa is estimated in CF layer. The uniform stress in Onyx layers is 13 MPa along the main length of the model. It is to be noted that the different values in tensile stress are within their respective individual limits of strength. Marforged® reports 36 MPa stress at yield for the pure Onyx matrix and tensile strength of 700 MPa for CF. The 0.9% strain is also well below the 1.5% strain at break reported by Marforged®.

Table 7. FE model results from tensile model.

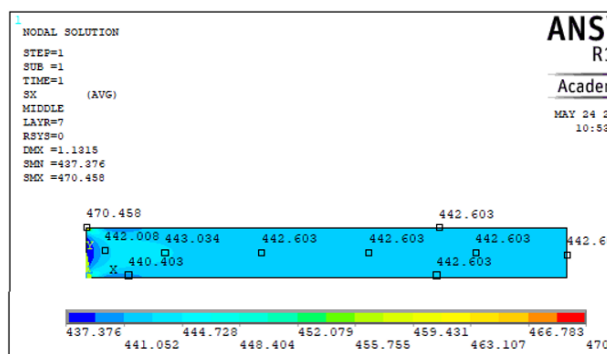| Description	Nodal solution	Units
Displacement UX	1.13	mm
CF: SX, Tensile stress	443	MPa
Onyx: SX, Tensile stress	13.2	MPa
Max longitudinal strain	0.009	mm/mm

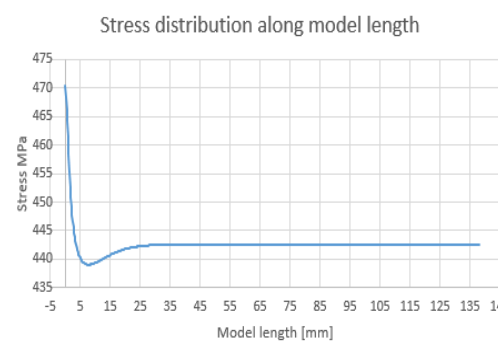**Figure 9.** Tensile stress in CF layer

Figure 10. Tensile stress distribution in CF layer.

3.4. FEA results from flexural model

The total load at mid-span was 303 N generating a maximum deflection of 7.6 mm. From the lowest CF-layer (layer 5) at mid-span of the beam, a maximum flexural stress of 445 MPa and equivalent stress

of 450 MPa was estimated. Moreover, the surface of the first Onyx layer (1st layer from bottom) was subjected to a flexural stress of 37 MPa and equivalent stress of 34 MPa. Marforged® reported flexural strength of 81 MPa for pure Onyx and 470 MPa for pure CF, thus no yield is to be expected in the Onyx layers [18]. The distribution of the flexural stress (SX) at the mid-span of the FE-model is presented in Figure 11. Furthermore, maximum stress values for selected layers at the mid-span are presented in Table 9.

Table 8. Results from flexural FE model at the mid-span of the beam.

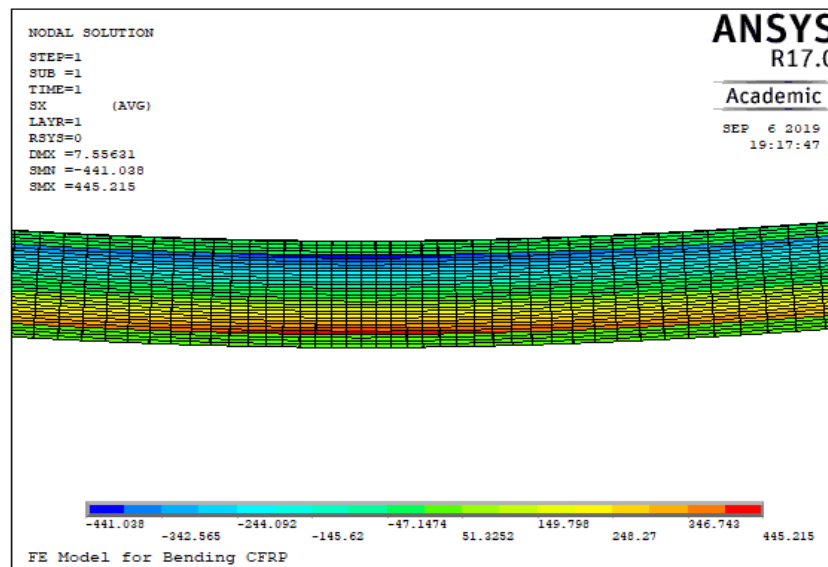| Description	Nodal solution	Units
Max. disp.,UZ	7.6	mm
CF: SX, Flexural stress	445	MPa
CF: SEQV, Von Mises Stress	450	MPa
Onyx: SX, Flexural Stress	37	MPa
Onyx: SEQV, Von Mises Stress	34	MPa
Max. strain, EPELX	0.012	mm/mm

Figure 11. Max Stress at the mid-span of flexural Model.

A summary of results from experiment, ROM and FEA are presented in Table 10, both for tensile and flexural samples. The fiber volume fraction estimated from experimental samples is used in ROM calculations. In the FEA the values are taken from the mid-span of the models. The FE result for the tensile and flexural was obtained from layer 7 and 5, respectively. Both layers are made from CF.

Table 9. Flexural stress from some layers of the FE model at the mid-span.

Layers →	L-1	L-2	L-3	L-4	L-5	L-6	L-12	L-13	L-14	L-17
Material	Onyx	Onyx	Onyx	Onyx	CF	CF	CF	CF	CF	onyx
Stress: SX [MPa]	37	34	31	29	445	390	170	134	97	0
Node nr.	1391	1391	1391	1391	1391	1391	1391	1391	1391	1445
Deflection, [mm]	7.6	-	-	-	-	-	-	-	-	-
Strain: EPLX	0.011	0.011	0.010	0.009	0.008	0.008	0.003	0.003	0.002	0.0

Table 10. Results of the composite samples from ROM, experimental test and FEA.

Description	Tensile stress [MPa]	Flexural Stress [MPa]
Experimental	560	271
ROM	453	244
FEA of CF: SX	443	445
FEA of Onyx: SX	13.2	37

4. Discussion

In the experiment, delamination failure was observed in both flexural (Figure 8) and tensile test (Figure 6) samples. The delamination was observed between the matrix and fiber layers and the matrix material was easy to peel off from the fiber. Also, it had been observed formation of voids between layers on both matrix- and fiber- materials during fabrication of samples. The delamination was probably due to the nature of AM, specifically weak bonding between successive layers. Referring to the tensile tests, all the tensile specimens fail within the gauge length close to the grip in CF layers (Figure 6). After successive longitudinal delamination of the samples, the failures at final stage were characterized in all cases as typical brittle failures with a sudden and strong energy release. The estimated tensile strength of 560 MPa and an E-modulus of 25 GPa, was obtained from the experimental tensile test. From flexural test results, the flexural strength of 271 MPa and E-modulus of 16 GPa was obtained. The bending samples failed at the mid-span and a delamination between fiber and matrix layers were observed in the samples (Figure 8).

In the FE-model it was assumed orthotropic material properties for the CF layers: Some material data was provided by Markforged®, while the rest of the material properties are estimated from AS4 carbon yarn as presented on Table 3. Poisson's ratio of Onyx were estimated from our tests based on five samples, fabricated in our lab.

FE- model with layered shell elements based on its idealized assumptions predict accurate values of stress in each composite layer. A significant deviation from the physical samples at critical levels of strain is the no-slip condition between the layers in the FE-model vs. delamination experienced in the test samples. The idealized geometry with no voids and perfectly arranged layers in the FE-model, compared to assumed voids and imperfections in the physical samples introduce further errors when predicting failure with FE-models. FEM is versatile tool for the understanding of the elastic properties of composite materials and the modeling can be further improved. Failure criteria e.g. Tsai-Wu criteria can be implemented but should be based on experimental data.

5. Conclusion

A delamination failure was the common cause of failure mainly in the tensile test. Bonding between successive non-identical material layers and adjacent layers of CF was weak. In contrast to all, the composite material provided a promising property with about 560 MPa in tensile strength and about 271 MPa in flexural strength, respectively. Furthermore, the UD composite material achieved an elastic modulus of 25 GPa and 16 GPa in tensile and bending, respectively.

References

[1]. Hull, D and Clyne T W 1996 *An introduction to composite materials* 2nd Ed. (Cambridge University Press) p 344.

[2]. Van Der Klift, Koga, F Y, Todoroki A, Ueda M, Hirano Y, and Matsuzaki R 2016 *Open J. Compos. Mater.* **6** (1) 18-27.

[3]. Ning F, Cong, W, Qiu J, Wei J, and Wang S 2015 *Composites Part B* **80** 369-78.

[4]. Jiang D and Smith D E 2017 *Addit. Manuf.*, **18** 84-94.

[5]. Strong, A B 2008 *Fundamentals of composites manufacturing: materials, methods and applications* 2nd Ed. (Society of Manufacturing Engineers) p 599.

[6]. Miracle D B, Donaldson S L et al. 2001 *ASM handbook Volume 21: Composites* 21 Ed. (ASM international) p 1201.

[7]. Hart R J, Patton E G and Sapunkov O 2018 *Characterization of continuous fiber-reinforced composite materials manufactured via fused filament fabrication*. Technical report, available at: https://apps.dtic.mil/dtic/tr/fulltext/u2/1062410.pdf. (Accessed: 20.10.2019].

[8]. Caminero M, Chacón J, García-Moreno I and Reverte J 2018 *Polym. Test.*, **68** 415-23.

[9]. Dickson A N, Barry J N, McDonnell K A and Dowling D P 2017 *Addit. Manuf.*, **16** 146-52.

[10]. Schwartz M M 1984 *Composite materials handbook* Ed. (McGraw-Hill) p 651.

[11]. Gay D and Hoa S V 2007 *Composite materials: design and applications* 2nd Ed. (CRC press) p 545.

[12]. Nicolais L, Meo M and Milella E 2011 *Composite materials: A Vision for the Future* 1st Ed. (Springer Science & Business Media) p 218.

[13]. Lozada J N, Ahuett-Garza H, Castañón P O, Verbeeten W M and González D S 2019 *Addit. Manuf.*, **26** 227-41.

[14]. Campbell F C 2010 *Structural composite materials* Ed. (ASM international) p 612.

[15]. Lee C, Kim S, Kim H and Ahn S 2007 *J. Mater. Process. Technol.*, **187** 627-30.

[16]. Barbero E J 2013 *Finite element analysis of composite materials using ANSYS®* 2nd Ed. (CRC press) p 366.

[17]. Markforged, *<Mark Two product specification.pdf>*. (Last accessed: 20.10.2019)

[18]. Markforged, *Onyx, material specification*. Available at https://www.3axis.us/matetials/markforged-materials.pdf (Last accessed: 20.10.2019)

[19]. Markforg3D, *<Markforged-Products-and-Applications.pdf>*. 2016.

[20]. Standard A, *ASTM D3039-Standard test method for tensile properties of polymer matrix composite materials*. 2008, ASTM International. p. 13.

[21]. Standard A J A S fT and Materials P: Philadelphia, USA 2007 D 7264/D 7264M-07 11.

[22]. Mac Donald, B.J. 2007 *Practical Stress Analysis with Finite Elements* 1st Ed. (Glasnevin Publishing) p 350.

[23]. Meddad, A, Azaiez J, Ait-Kadi A and Guenette R 2002 *J. Compos. Mater.*, **36** (4) 423-41.